Electronic supplementary (ESI) for:

Use of ionic liquids (ILs) for the IL-anion size-dependent formation of Cr, Mo and W nanoparticles from metal carbonyl $M(CO)_6$ precursors

Engelbert Redel,[a] Ralf Thomann[b] and Christoph Janiak[a]*

[a] *Institut für Anorganische und Analytische Chemie, Universität Freiburg, Albertstr. 21, D-79104 Freiburg, Germany. Fax: int+49 761 2036147; Tel: int+49 761 2036127; E-mail: janiak@uni-freiburg.de*

[b] *FMF (Freiburger Material Forschungszentrum),Universität Freiburg, Stefan-Meier-Str. 21, D-79104 Freiburg, Germany, Tel: int+49 761 2035379; E-mail: ralf.thomann@fmf.uni-freiburg.de*

Materials and instrumentation:
$M(CO)_6$ (M = Cr, Mo, W) were obtained from Aldrich and Merck, ionic liquids from IoLiTec (H_2O content << 100 ppm; Cl^- content << 50 ppm).
Metal carbonyls are poisoneous due to the possible liberation of CO and, thus, should be handled with care.
All manipulations were done using Schlenk techniques under argon since the metal carbonyls salts are hygroscopic and air sensitive. The ionic liquids were dried at high vacuum (10^{-3} mbar) for several days. Transmission electron microscopy (TEM) photographs were taken at room temperature from a carbon coated copper grid on a Zeiss LEO 912 transmission electron microscope operating at an accelerating voltage of 120 kV.

Nanoparticle synthesis:
In a typical experiment the metal carbonyl $M(CO)_6$ was dissolved/suspended under argon/air in the dried and deoxygenated ionic liquid. The solution was heated up to 230 °C for several hours to thermally decompose the metal carbonyl.
Thermal decompositions were carried out under argon (or air) in a vessel which was connected to an oil bubbler. In a typical experiment the metal carbonyl $M(CO)_6$ (M = Cr, Mo and W, 0.118, 0.078 and 0.057 g, respectively) was dissolved (~1 h) under argon at room temperature in 3.0 g of the ionic liquid to give a 1 wt% M solution. The solution was slowly heated up to 230 °C for 12 h under stirring. After cooling to room temperature under argon an aliquot of the ionic liquid was collected under argon atmosphere for *in situ* TEM and dynamic light scattering characterization.

Alternatively, the solution was irradiated at 200-450 nm for 15 min for photolytic decomposition of $M(CO)_6$.
Photolytic decompositions of a solution of $Mo(CO)_6$ (0.008 g) in 3.0 g $BMim^+BF_4^-$ were carried out in a Kürner UV 1000 reactor from Kürner-Analysentechnik in quarz tubes for 15 min under argon with a Hg-UV lamp (1000 W) in the range 200-450 nm.

Statistical graphs for dynamic light scattering (Fig. S1-S11)

A Malvern Zetasizer Nano-ZS was used for the dynamic light scattering measurements working at 633 nm wavelength. Care was taken for choosing the right parameters, such as the index of refraction of Cr, Mo and W at this wavelength. Samples were prepared by dissolution of 10 µL of the metal dispersion in the ionic liquid (1 wt% of M) in 2 mL *n*-butyl-imidazol (99 % p.a.; particle free). From this solution 75 µL were further diluted with 1.25 mL *n*-butyl-imidazol.

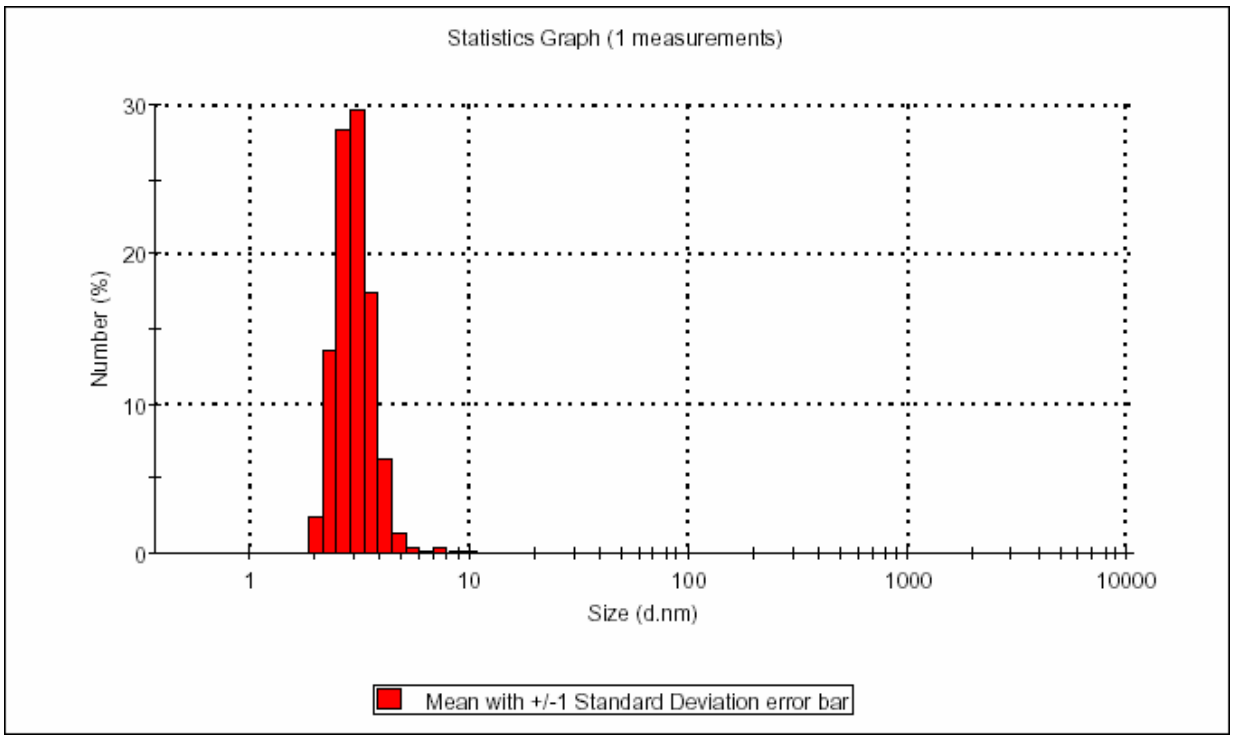

Fig. S1 Cr metal nanoparticles in $BMim^{+}BF_4^{-}$ (thermal decomposition)

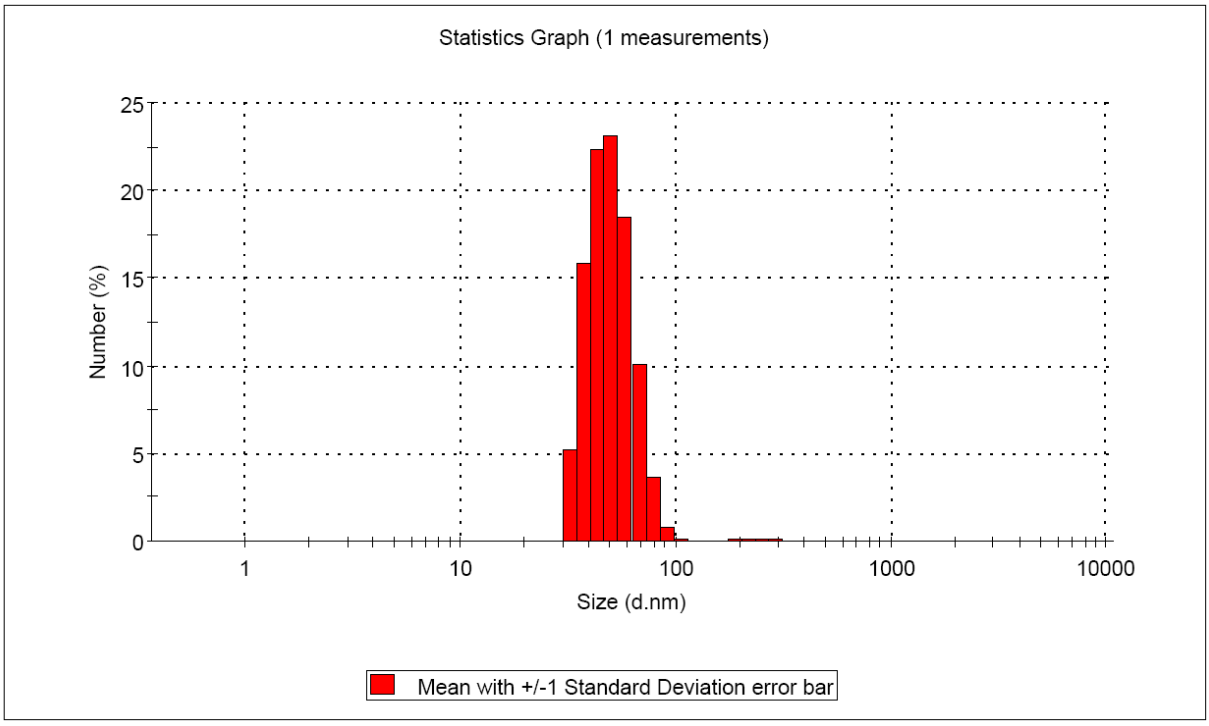

Fig. S2 Cr metal nanoparticles in $BtMA^{+}Tf_2N^{-}$ (thermal decomposition)

A fragmentation of larger to smaller particles may be induced by the Laser light.

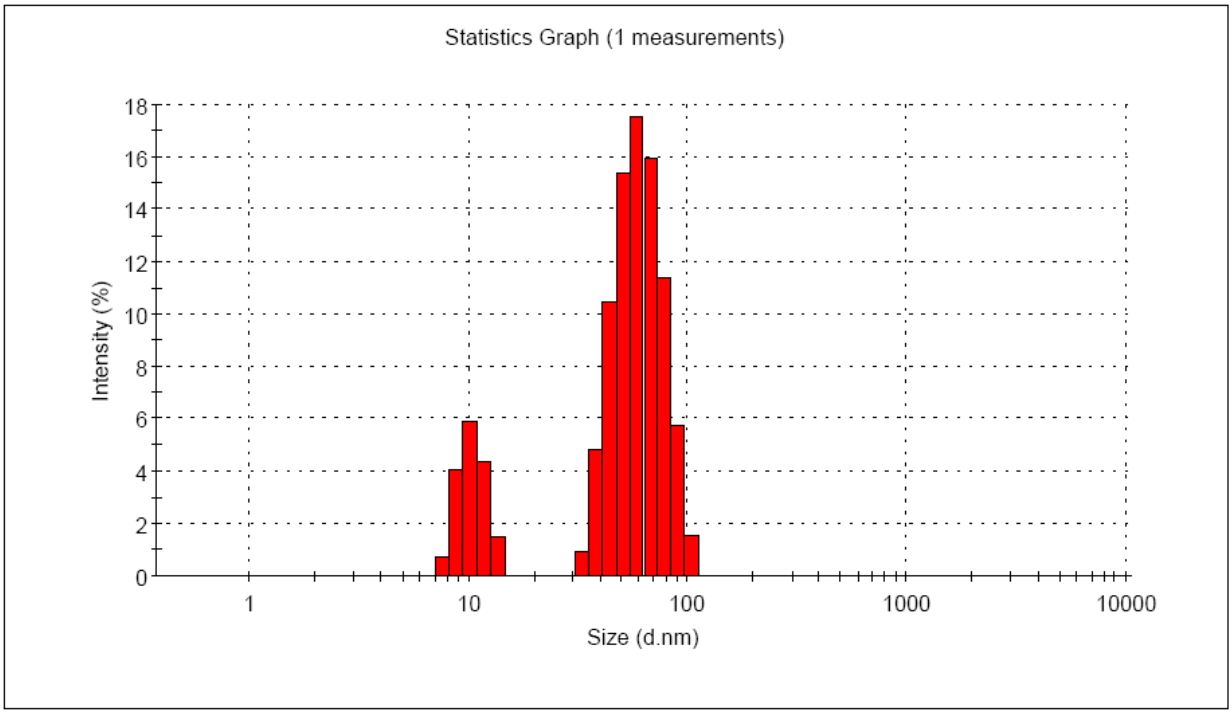

Fig. S3 Cr-oxide metal nanoparticles in $BtMA^{+}Tf_2N^{-}$ (thermal decomposition)
A fragmentation of larger to smaller particles may be induced by the Laser light.

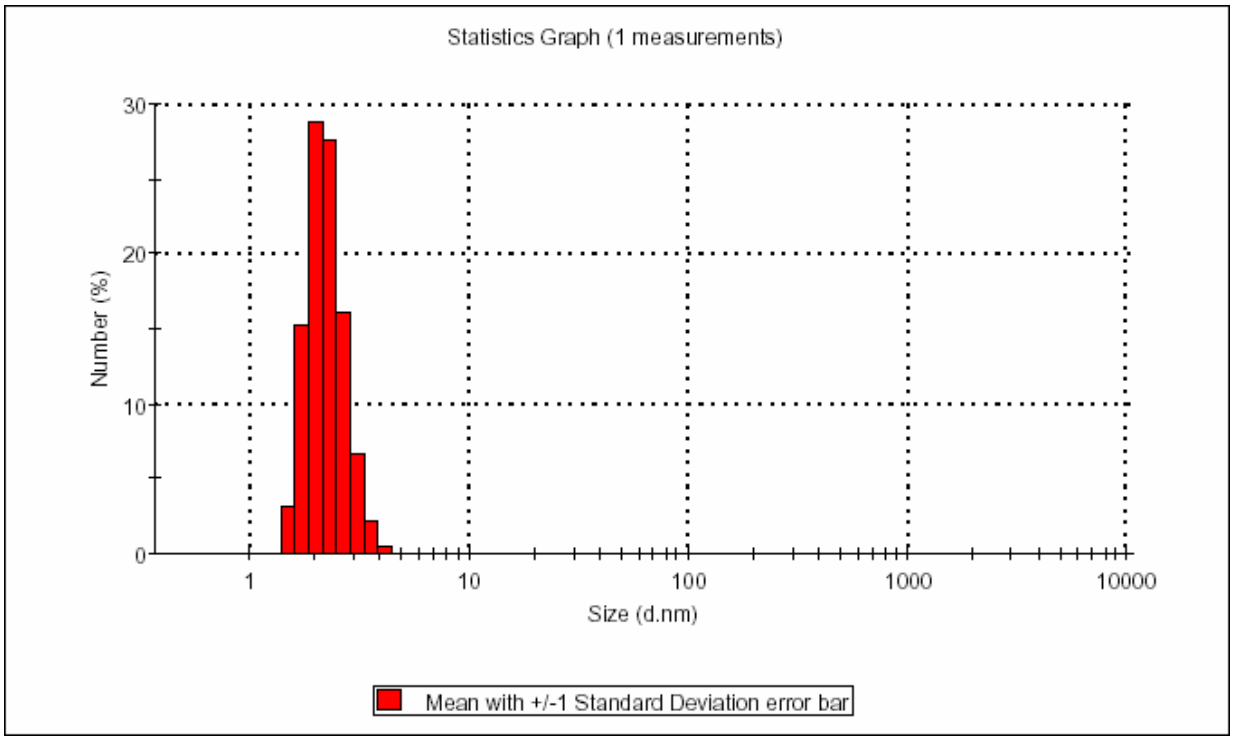

Fig. S4 Mo metal nanoparticles in $BMim^{+}BF_4^{-}$ (thermal decomposition)

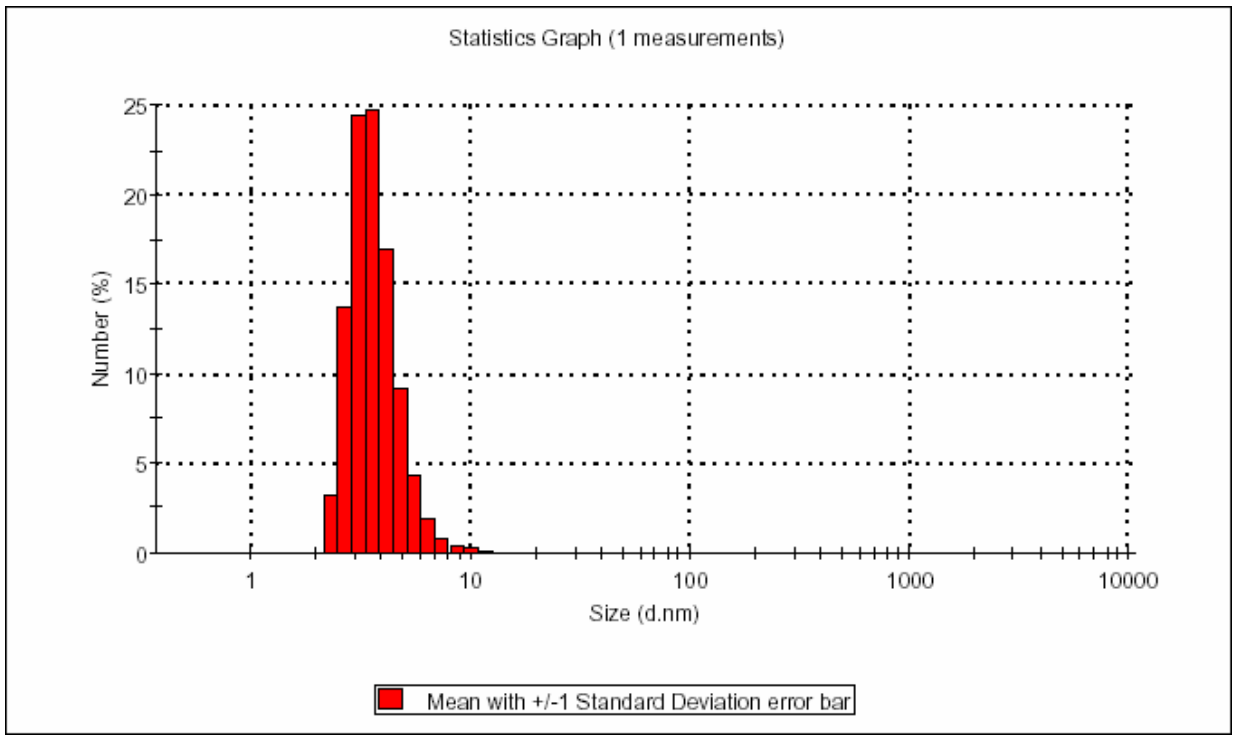

Fig. S5 Mo metal nanoparticles in $BMim^{+}BF_4^{-}$ (photolytic decomposition)

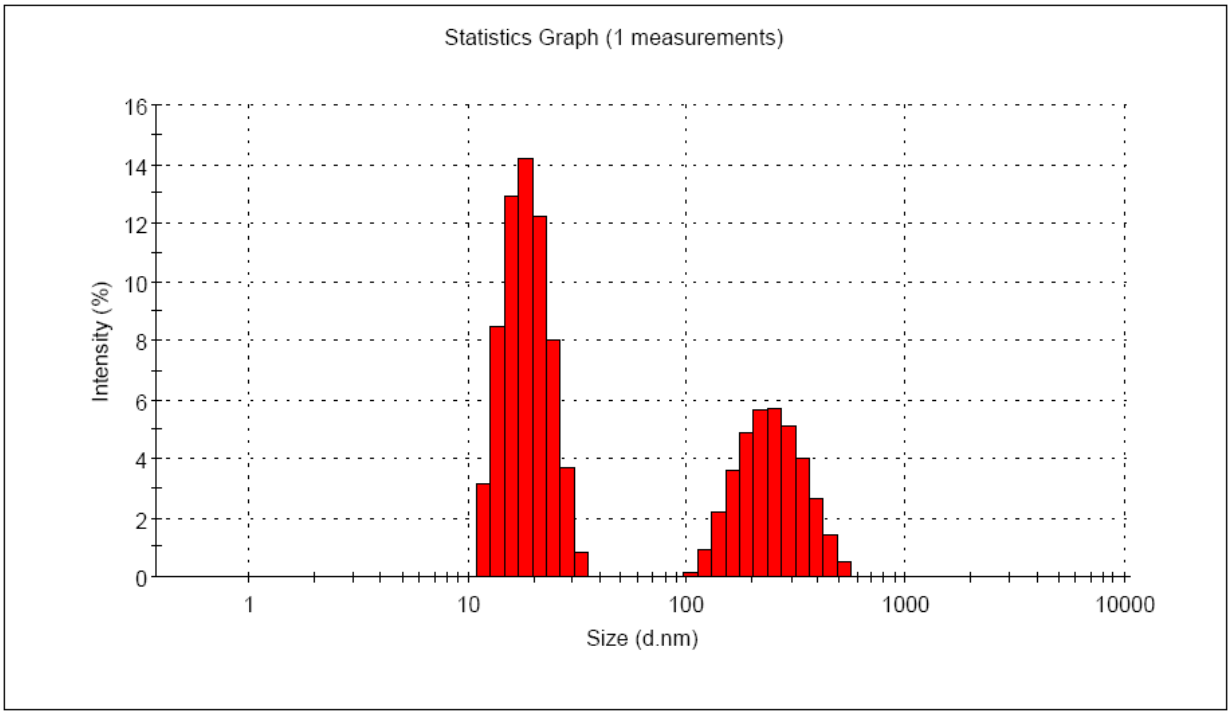

Fig. S6 Mo metal nanoparticles in $BtMA^{+}Tf_2N^{-}$ (thermal decomposition)

A fragmentation of larger to smaller particles may be induced by the Laser light.

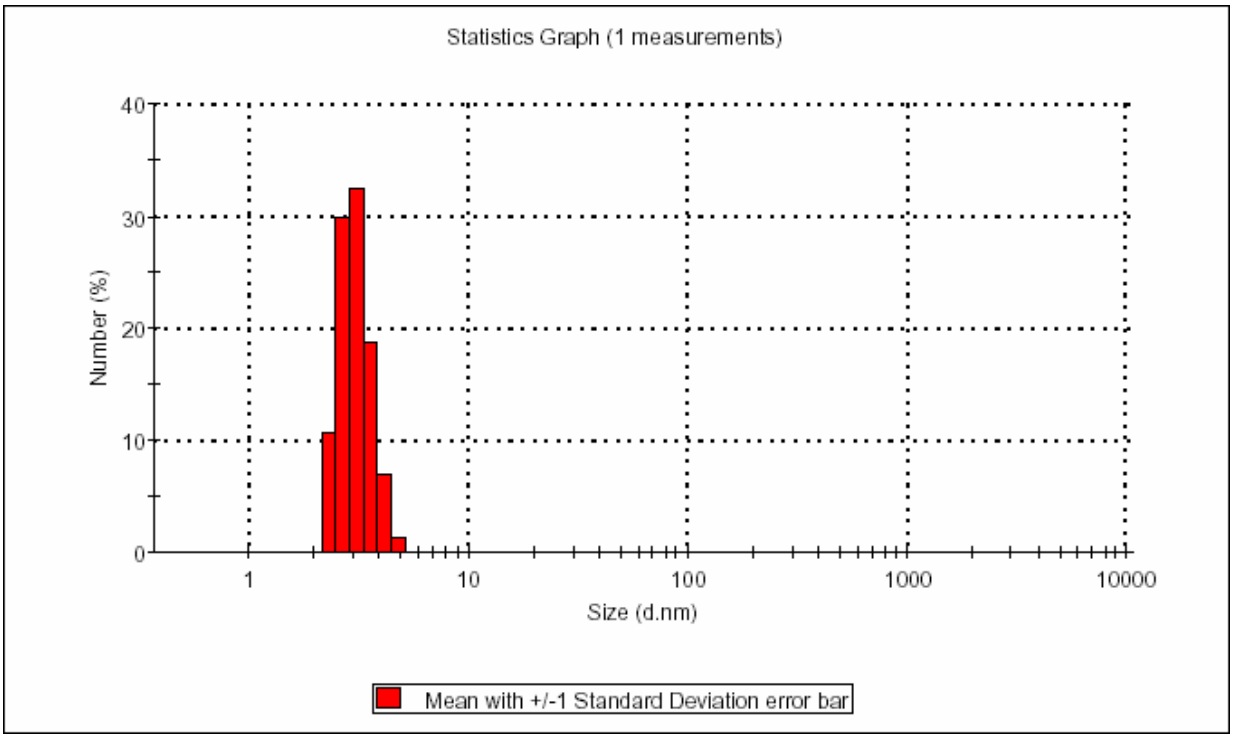

Fig. S7 W metal nanoparticles in $BMim^{+}BF_4^{-}$ (thermal decomposition)

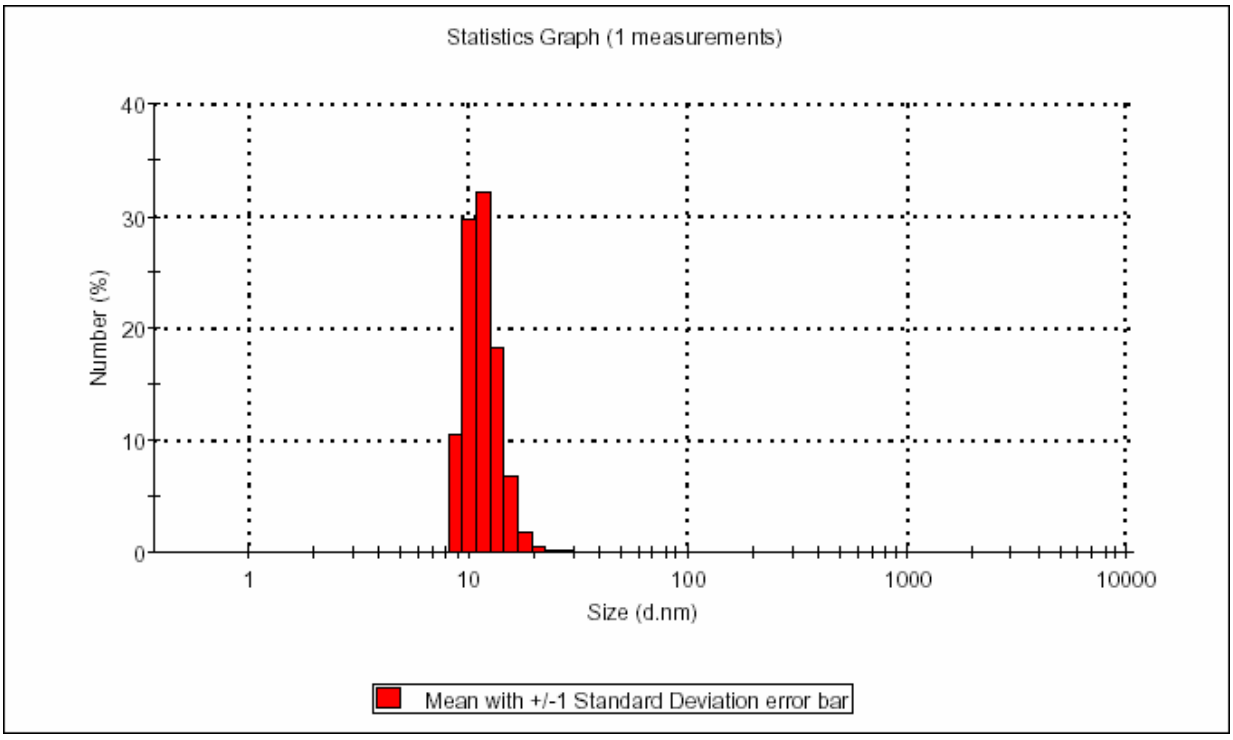

Fig. S8 W metal nanoparticles in $BMim^{+}OTf^{-}$ (thermal decomposition)

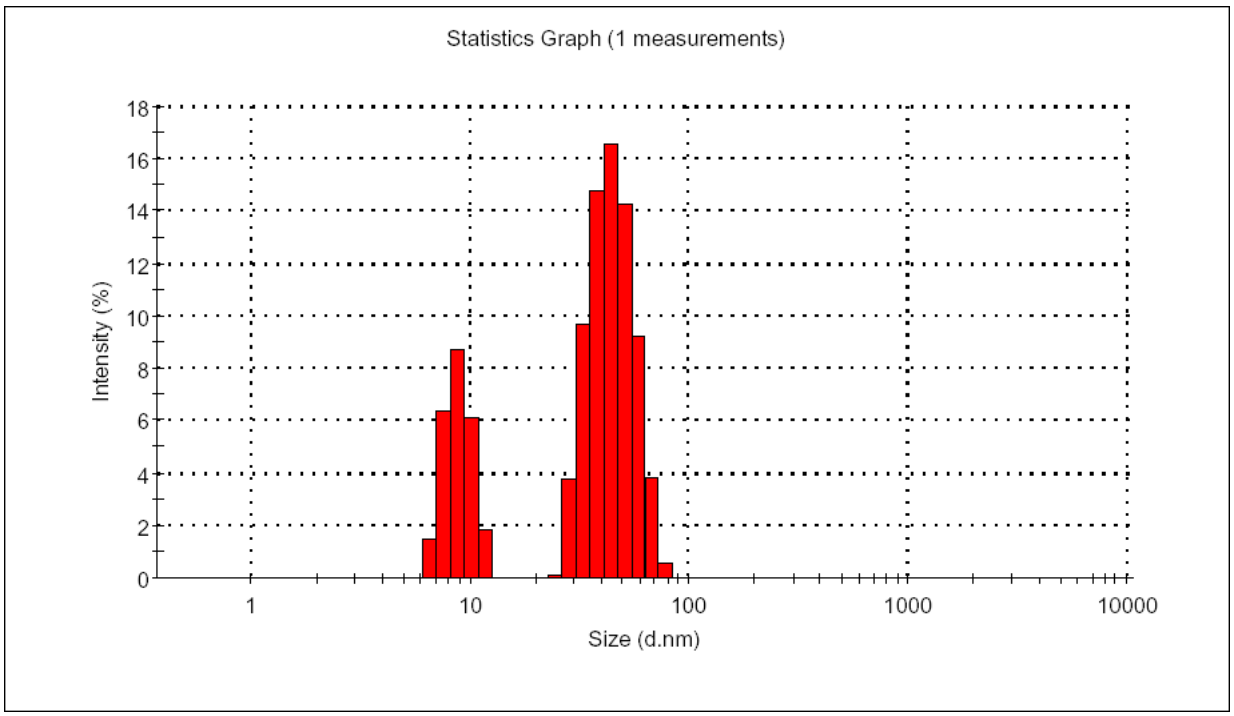

Fig. S9 W metal nanoparticles in $BMim^{+}NTf_2^{-}$ (thermal decomposition)

A fragmentation of bigger nanoparticles to smaller particles could be possible !

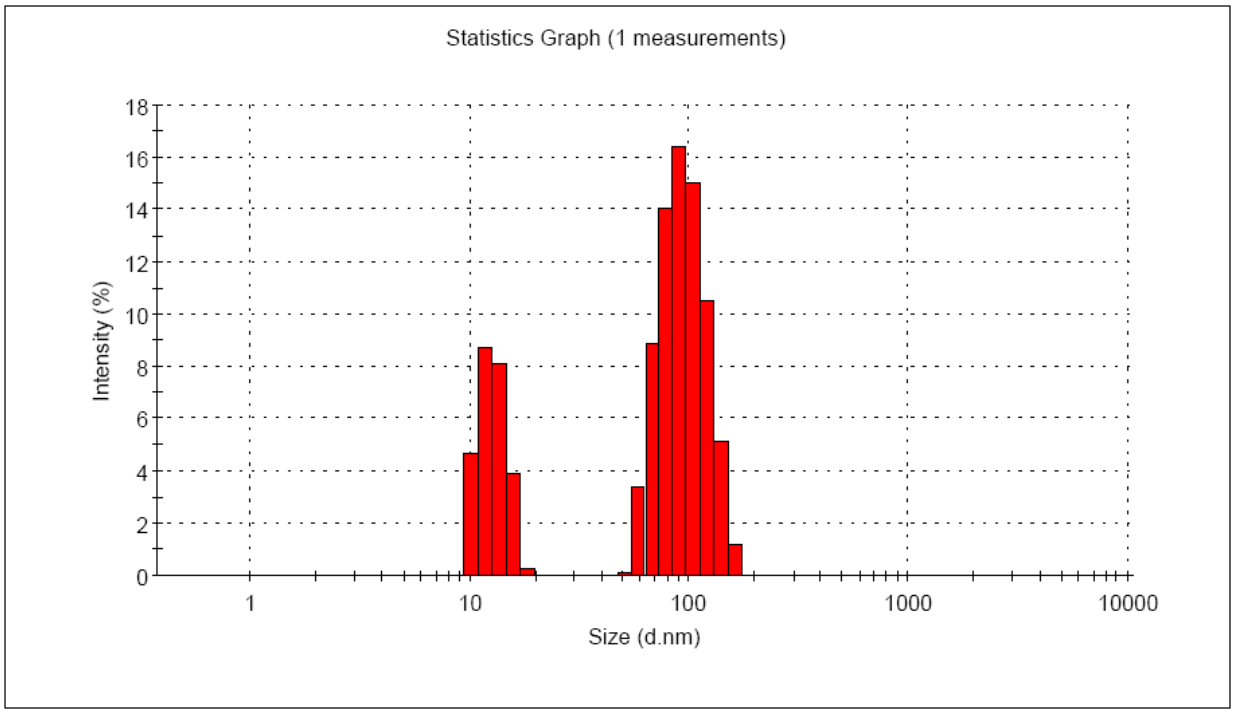

Fig. S10 W metal nanoparticles in $BtMA^{+}Tf_2N^{-}$ (thermal decomposition)

A fragmentation of larger to smaller particles may be induced by the Laser light.

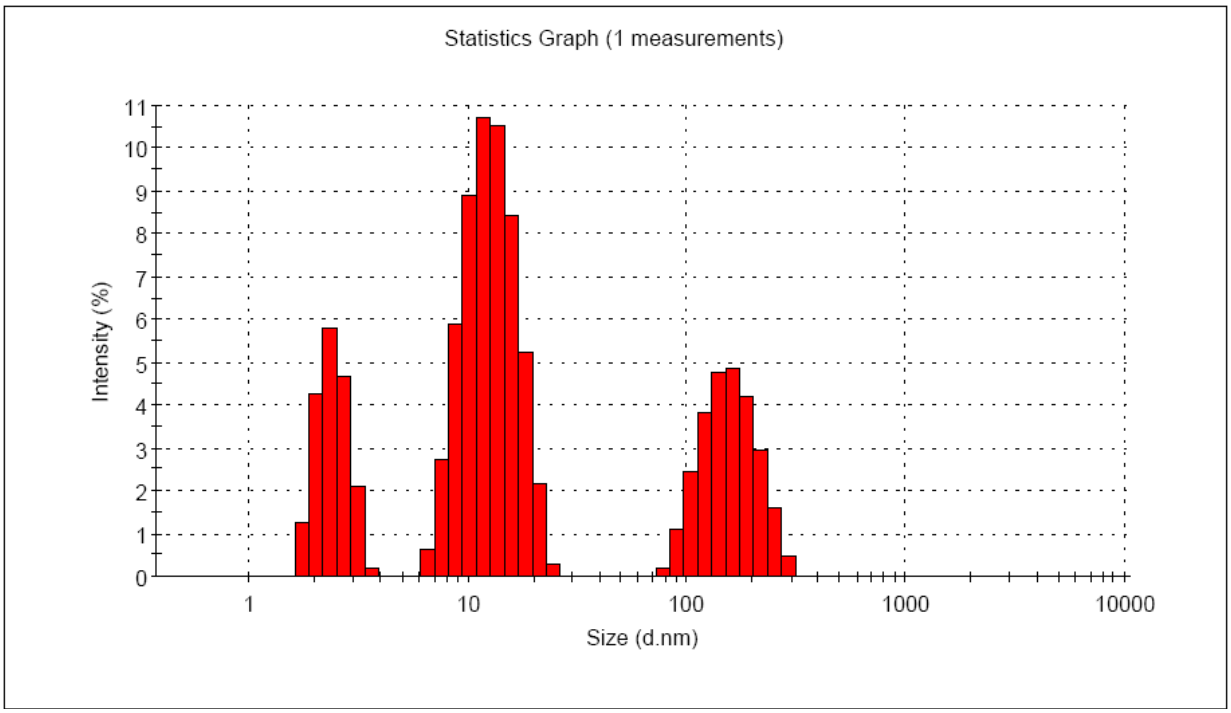

Fig. S11 W-oxide metal nanoparticles in $BtMA^{+}Tf_2N^{-}$ (thermal decomposition); the inhomogeneity agrees with the TEM-pictures

Additional transmission electron microscopy (TEM) and transmission electron diffraction (TED) pictures (Fig. S12-S24)

Transmission electron microscopy (TEM) and transmission electron diffraction (TED) photographs (Figures S11-S17) were taken at room temperature from a carbon coated copper grid on a Zeiss LEO 912 transmission electron microscope operating at an accelerating voltage of 120 kV. Samples were stored under argon before TEM or TED analysis, only on the short transfer time of about 1-2 sec they had contact to air, with the nanoparticles still be immersed in the protecting ionic liquid.
The black bar in the TED pictures is the beam stopper.
The red curve in the TED pictures represents the intensity profile along the vertical or horizontal red line. The distance between the maxima of a halo ring across the center gives the halo diameter (in µm) from which the lattice d-spacing can be calculated, according to 7.88/(diameter) = d (in nm).

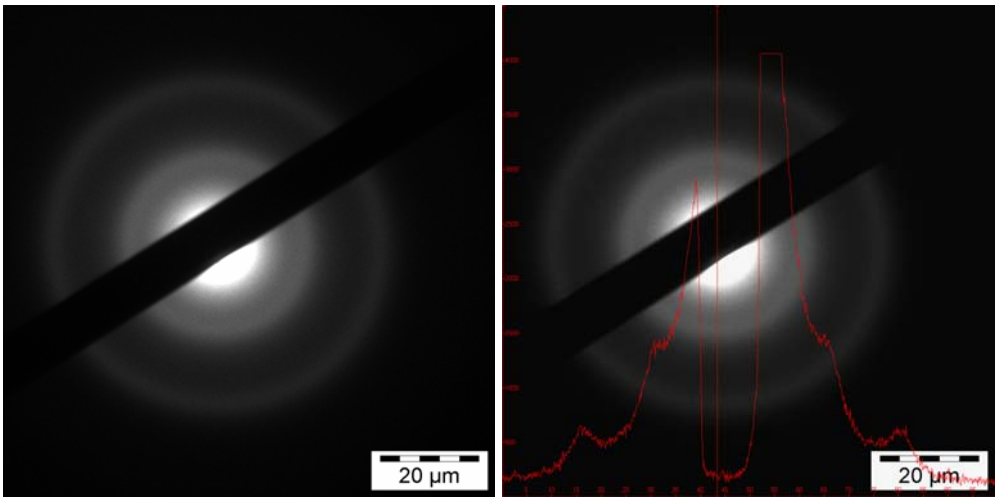

Fig. S12 TED photographs of carbon coated copper grid.

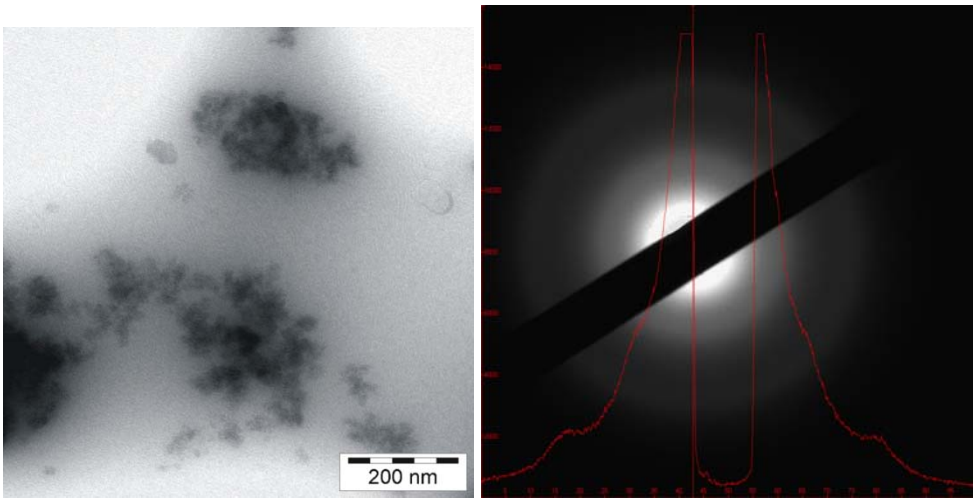

Fig. S13 TEM/TED photograph of small Cr metal nanoparticles in $BMim^{+}BF_4^{-}$ (thermal decomposition). TED shows only the carbon grid here, due to the amorphous character of the sample.

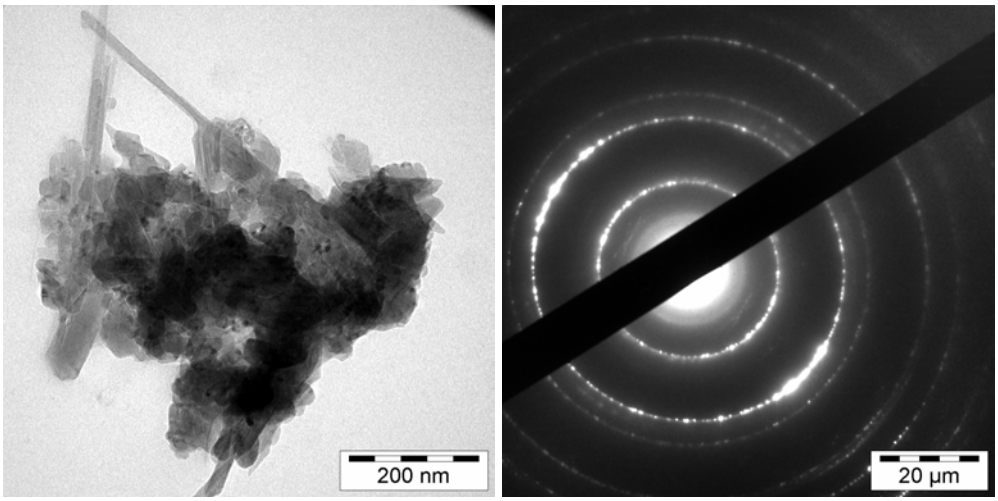

Fig. S14 TEM/TED photograph of crystalline Cr metal NPs in $BtMA^{+}Tf_2N^{-}$ (thermal decomposition). The D-values match with the D-spacing of Cr metal.

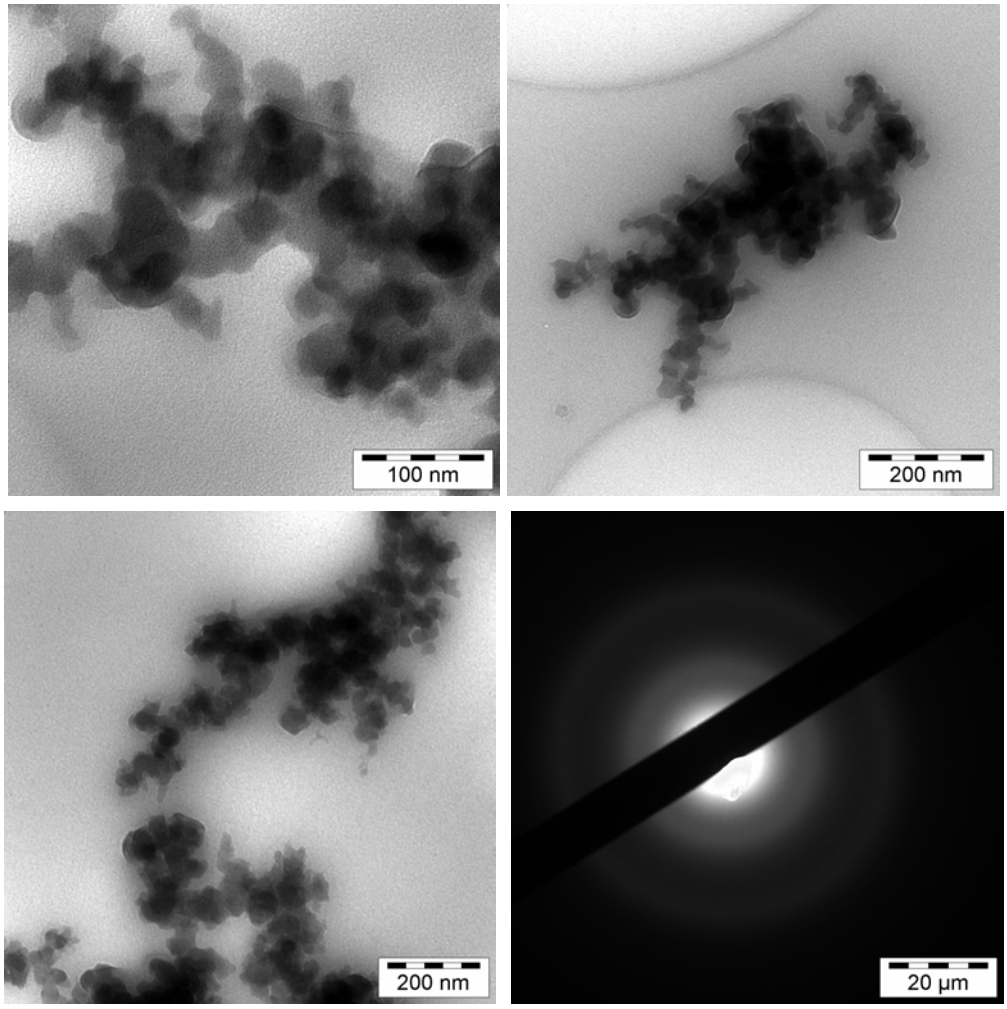

Fig. S15 TEM/TED photograph of Cr-oxide metal NPs in $BtMA^{+}Tf_2N^{-}$ (thermal decomposition). TED shows only the carbon grid here, due to the amorphous character of the sample.

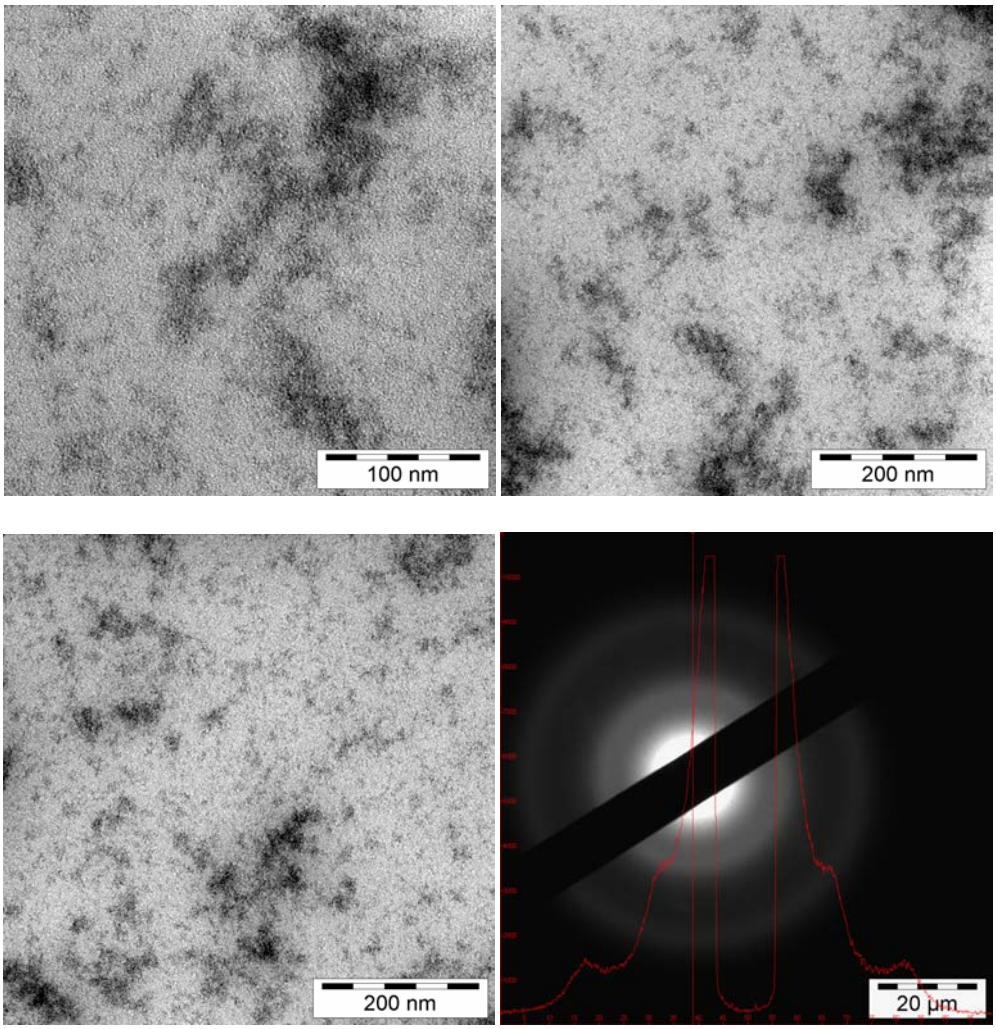

Fig. S16 TEM/TED photographs of small Mo metal nanoparticles in $BMim^{+}BF_4^{-}$ (**thermal** decomposition). TED shows only the carbon grid here, due to the amorphous character of the sample.

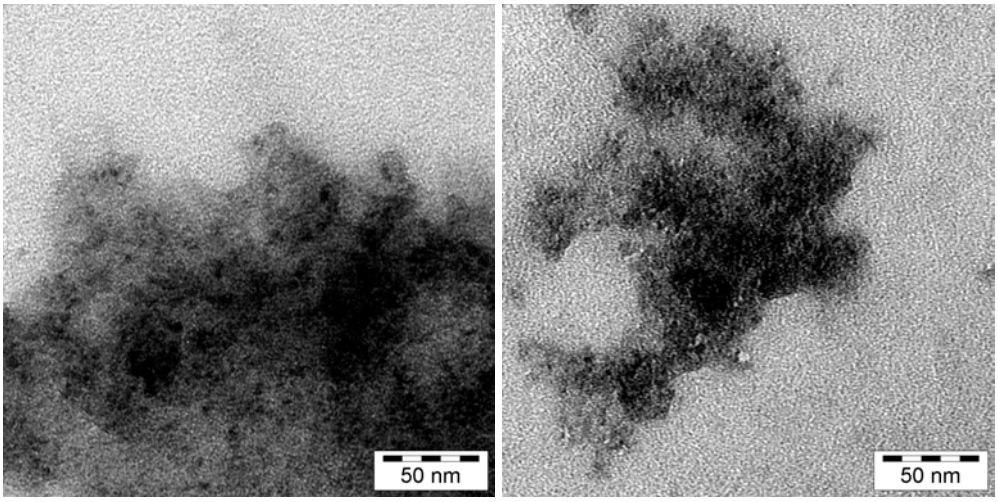

Fig. S17 TEM photograph of small Mo metal NPs in $BMim^{+}BF_4^{-}$ (**photolytic** decomposition).

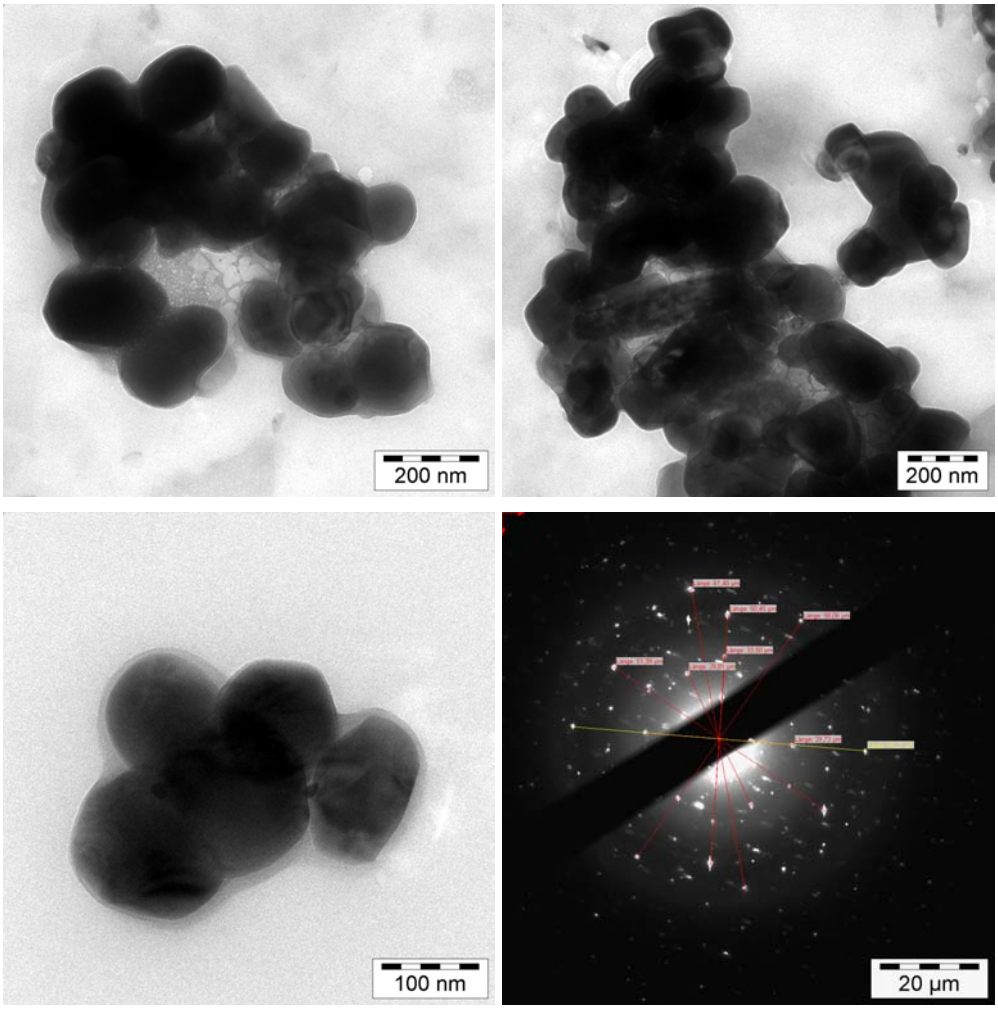

Fig. S18 TEM/TED photograph of crystalline Mo metal NPs in $BtMA^{+}Tf_2N^{-}$ (thermal decomposition). The D-values match with the D-spacing of Mo metal.

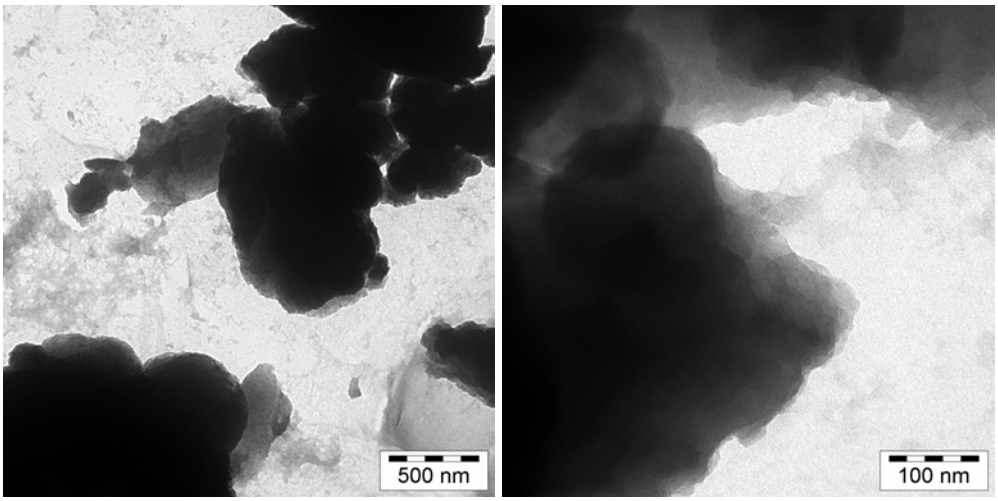

Fig. S19 TEM/TED photograph of Mo-oxide metal NPs in $BtMA^{+}Tf_2N^{-}$ (thermal decomposition).

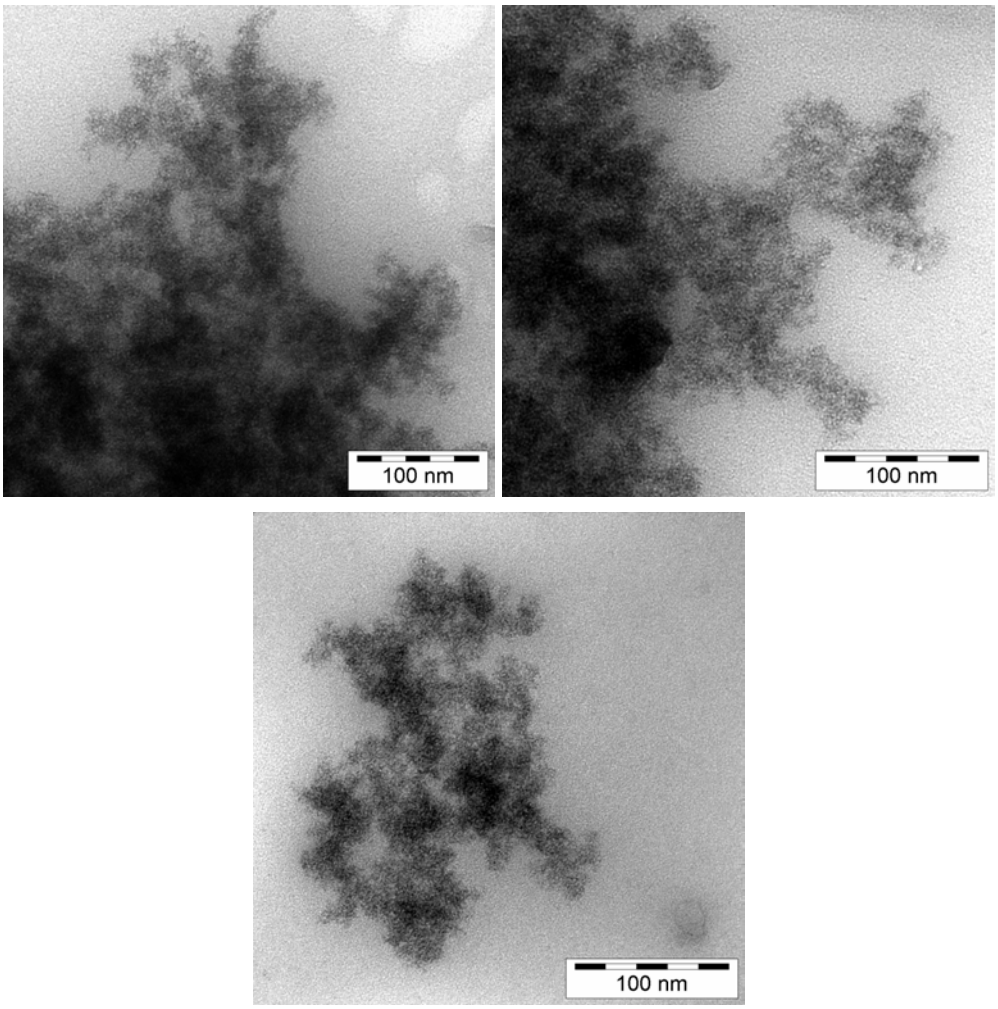

Fig. S20 TEM photographs of small W metal nanoparticles in **BMim$^+$BF$_4^-$** (thermal decomposition).

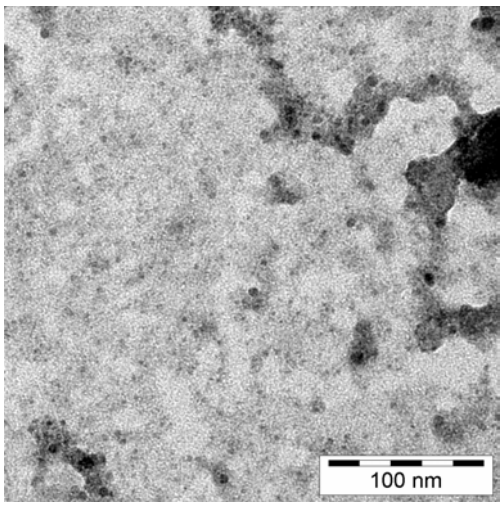

Fig. S21 TEM photograph of medium W metal nanoparticles in **BMim$^+$OTf$^-$** (thermal decomposition)

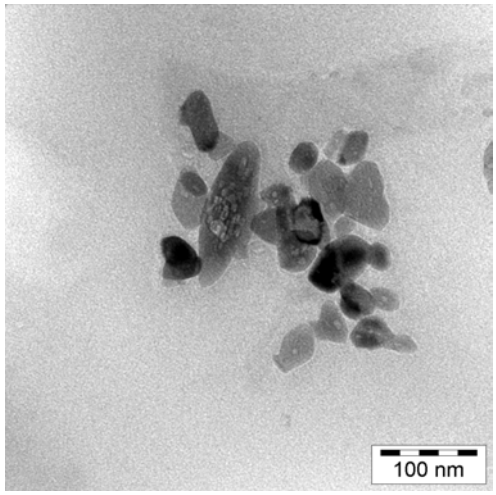

Fig. S22 TEM photograph of W nanoparticles from $W(CO)_6$ in $BMimNTf_2$ (thermal decomposition.

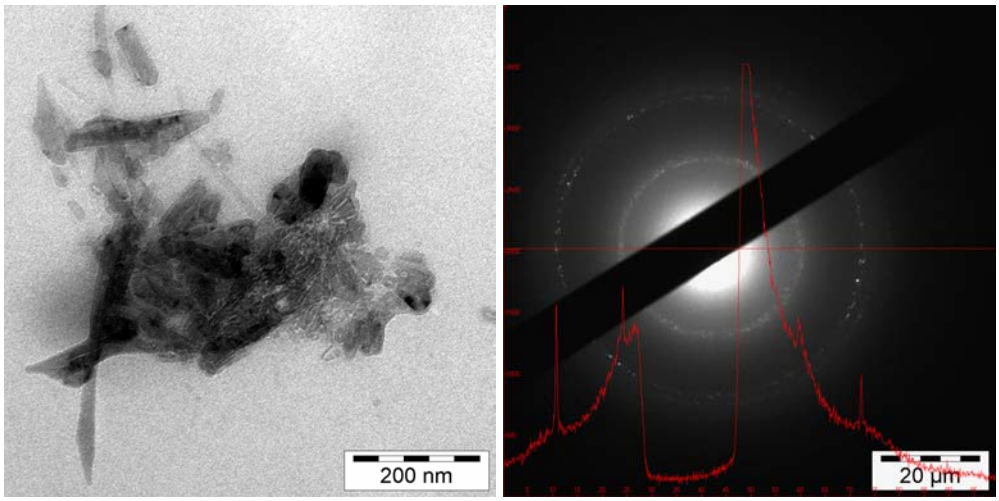

Fig. S23 TEM/TED photograph of crystalline W metal NPs in $BtMA^+Tf_2N^-$ (thermal decomposition).

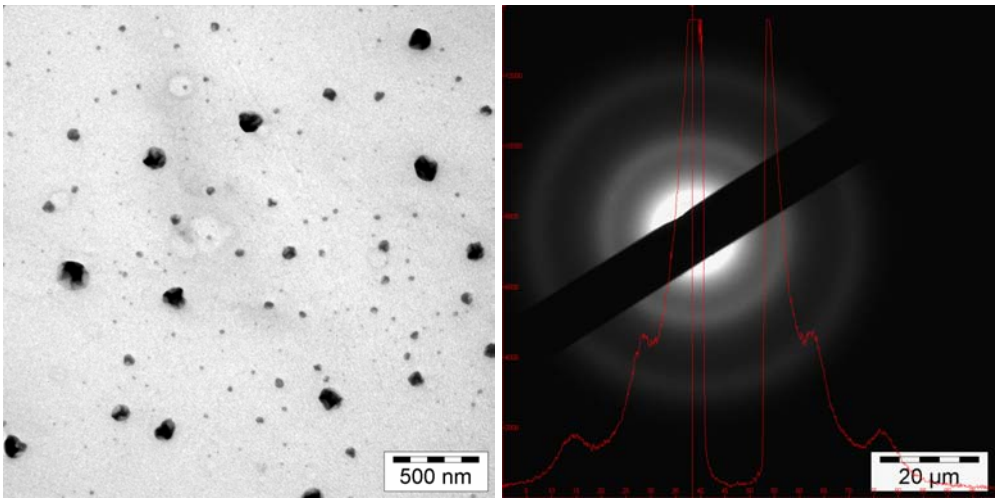

Fig. S24 TEM/TED photograph of W-oxide metal NPs in $BtMA^+Tf_2N^-$ (thermal decomposition). TED shows only the carbon grid here, due to the amorphous character of the sample.

Photographs of synthesized metal and metal oxide nanoparticle dispersion in ionic liquids (metal = Cr, Mo, W) (Fig. S25-S27)

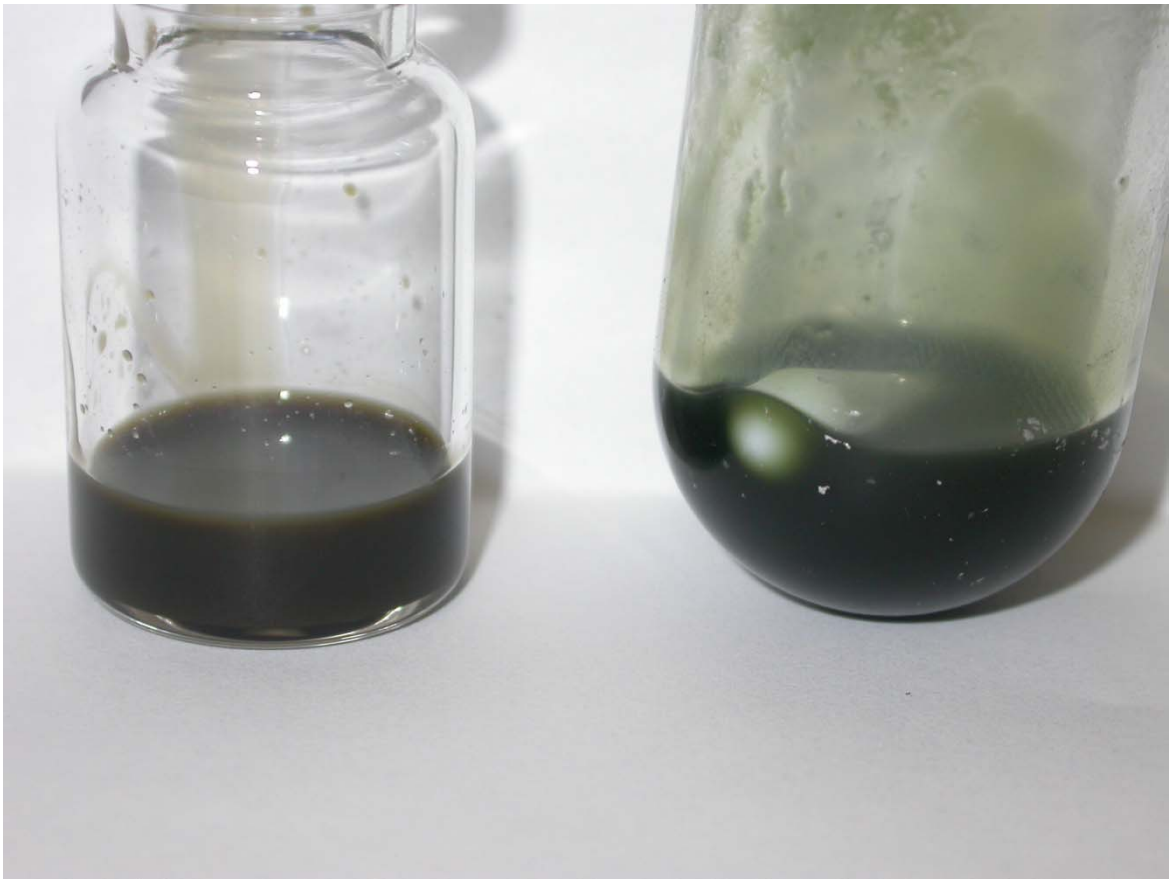

Fig. S25 Dispersion of brownish Cr-oxide (left) and dark-green Cr metal (right) NPs in $BtMA^{+}Tf_2N^{-}$.

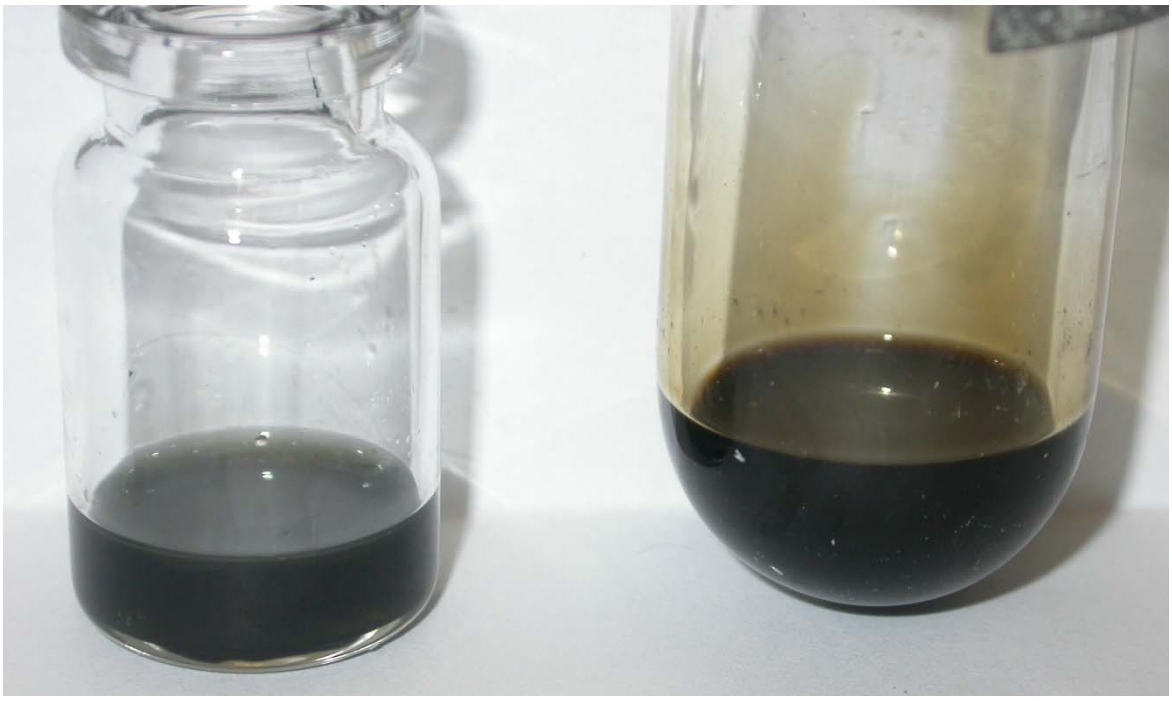

Fig. S26 Dispersion of gray-black Mo-oxide (left) and brown Mo metal (right) NPs in $BtMA^{+}Tf_2N^{-}$.

Fig. S27 Dispersion of brown W-oxide (left) and gray-blue W metal NPs (right) in $BtMA^{+}Tf_2N^{-}$.